**Proceedings of the 12th Asian Congress of Fluid Mechanics**
**18-21 August 2008, Daejeon, Korea**

# Mechanisms of Core Perturbation Growth in Vortex-Turbulence Interaction

F. Hussain*[1] and D. S. Pradeep*[2]

*[1] Department of Mechanical Engineering, University of Houston, Houston, TX, USA, fhussain@uh.edu
*[2] Department of Mechanical Engineering, University of Houston, Houston, TX, USA

**ABSTRACT:** We study mechanisms of coherent structure decay via direct numerical simulations (DNS) of a vortex column interacting with external, fine-sale turbulence. Ensemble-averaged statistics show growth of strong core (Kelvin) waves induced by the external turbulence - surprising, given the stabilizing effect of rotation in the vortex core. We explore two potential mechanisms of perturbation growth and core transition: (i) resonant forcing of Kelvin waves by turbulence filaments wrapping the column, and (ii) growth of optimal *transient* perturbations. We demonstrate the possibility of ring-vortex wave resonance even for relatively weak rings. Resonance in the form of amplifying core dynamics results in sheath-like structures in the core, known to be unstable to a Kelvin-Helmholtz-like instability. However, this process requires sustained organized ring-like structures over several vortex turnover times. Amplification of core perturbations in optimal transient modes also occurs through resonant forcing. Several orders of magnitude growth is possible at even moderate $Re$ ($\sim 10^4$) before the inevitable (linear) decay. We briefly examine the nonlinear evolution of optimal bending modes and show that such growth reproduces features of vortex interaction with turbulence: enhanced core diffusion, core perturbation growth, and circulation overshoot. Results from transient growth analysis suggest the importance of optimal transient modes in governing the decay of turbulent vortices.

## 1. FLOW EVOLUTION

Consider an isolated, temporally-evolving vortex column periodic along the axias. DNS uses a modified version of the Fourier pseudospectral method. Simulations are initialized by superposing the vorticity fields corresponding to a laminar vortex column and a radially compact region of random, fine-scale fluctuations. The turbulence adjusts to the presence of the mean flow within a few vortex turnover times. In this transient period, a large fraction of the three-dimensional energy rapidly cascades to smaller scales, then dissipated. Consequently, the turbulence kinetic energy TKE (figure 1$c$) decreases sharply at early times, before settling in to a period of slower decay. The figure plots TKE normalized by the instantaneous mean velocity and length scales ($v_1$ and $r_1$). TKE decays faster than the vortex, and suggests that the flow does not attain an equilibrium (self-similar) state even after several hundred turnover times, $T$. By $T = 400$, the flow is nearly laminar, with most of the fluctuation energy located within the vortex core. While core fluctuation energy in this case decays monotonically, this is not necessarily the case for other parameter values or initial conditions. Turbulence both within and outside the core may experience temporary amplification, as discussed later.

Figure 2 plots results for $u'$, $v'$, $w'$ (radial, azimuthal, and axial velocity fluctuations) and the Reynolds stress for an ensemble of 20 simulations. All plots are at the same stage of evolution. The ensemble is generated with different random initial conditions for the turbulence, but with all parameters held constant. There is strong growth of core turbulence energy, with small variations of turbulence intensity amplitudes within the the vortex core. In contrast, the Reynolds stress shows a sharp distinction between the core and outside. It varies little among different realizations outside the core, but shows a large scatter (with nearly zero mean when averaged over all realizations) within the core.

The simultaneous occurrence of large fluctuation intensities and negligible Reynolds stress within the core is due to the dominance of wave-like motions therein. The velocity perturbations (over a wide range of axial and azimuthal wavenumbers) induced by the external threads trigger a set of

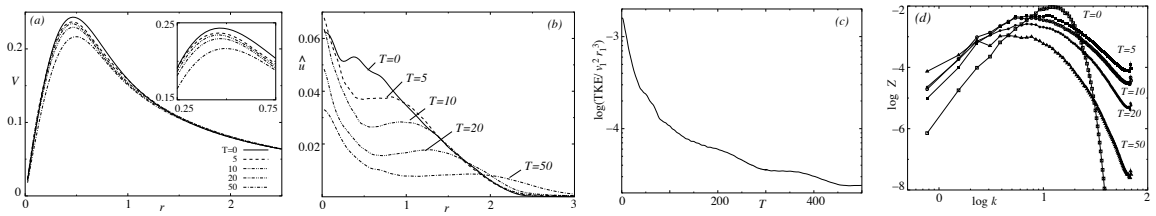


Figure 1: ($a$) Profiles of mean azimuthal velocity $V$ at early times of evolution; inset shows the profiles in the vicinity of $r_1$. ($b$) Profiles of turbulence intensity $\widehat{u}$. ($c$) Evolution of volume-integrated turbulence kinetic energy, scaled by mean velocity peak $v_1$. ($d$) Enstrophy spectra $Z(k)$ at early times of evolution, when resolution requirements are the most stringent.

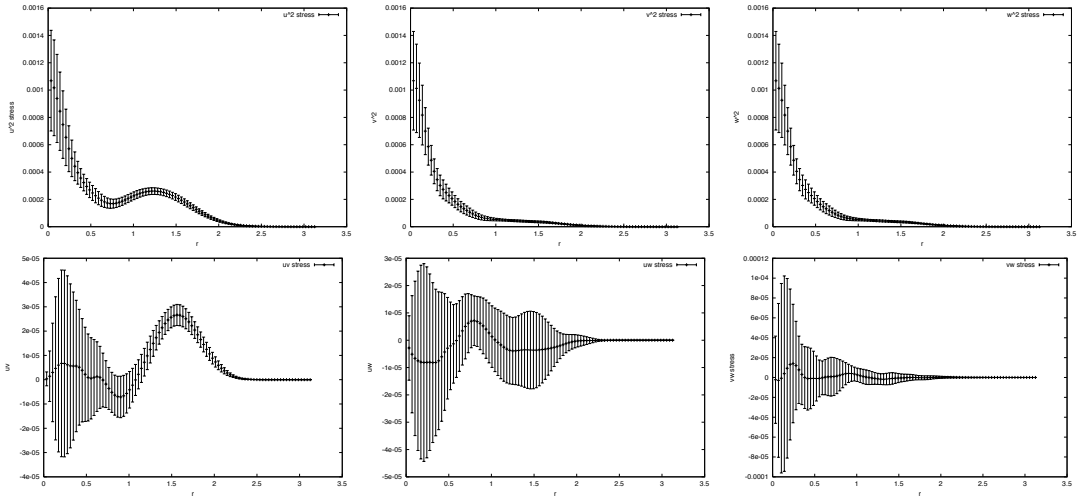


Figure 2: Components of the Reynolds stress tensor at $T = 15$: ($a$) $\overline{u'^2}$, ($b$) $\overline{v'^2}$, ($c$) $\overline{w'^2}$, ($d$) $\overline{u'v'}$, ($e$) $\overline{u'w'}$, and ($f$) $\overline{v'w'}$. Averages obtained over $\theta$, $z$ and 20 realizations. Error bars denote r.m.s. deviation from mean.

Kelvin waves within the core. To understand how core fluctuations amplify, we consider two potential mechanisms in the following sections. First, we idealize the turbulent flow as an array of axisymmetric vortex rings surrounding the column. We examine whether relatively weak rings can trigger large-amplitude waves in the core through resonant forcing. Second, we pursue transient growth analysis to study the evolution of the largest growing initial perturbations.

## 2. TURBULENCE-INDUCED VORTEX CORE DYNAMICS (CD)

We construct an idealized flow: a rectilinear vortex column surrounded by an array of identical vortex rings, coaxial with the column. The key parameters characterizing the flow are the ring-to-column circulation ratio $\gamma = \Gamma_R/\Gamma_C$, where $\Gamma_R$ is the circulation of a single ring and $\Gamma_C$ the column circulation, and the vortex Reynolds number $Re \equiv \Gamma_C/\nu$, where $\nu$ is the kinematic viscosity. The initial condition is shown schematically in Figure 3($a$). To examine the possibility of resonance, we look for those values of $\gamma$ and $\lambda$ where the axial advection velocity of an individual ring matches the wave-speed of core dynamics (CD) in the column.

Figure 3($c$) shows core wavespeed and ring speed as functions of $\lambda$. With decreasing $\lambda$, ring velocity increases monotonically. This is due to the increasing contribution from mutually-induced motions, as illustrated in Figure 3($b$). The ring at $z_A$ contributes positive $u_z$ and negative $u_r$ at the center of the neighboring ring at $z_B > z_A$. The radial velocity contribution at $B$ is canceled by an equal positive

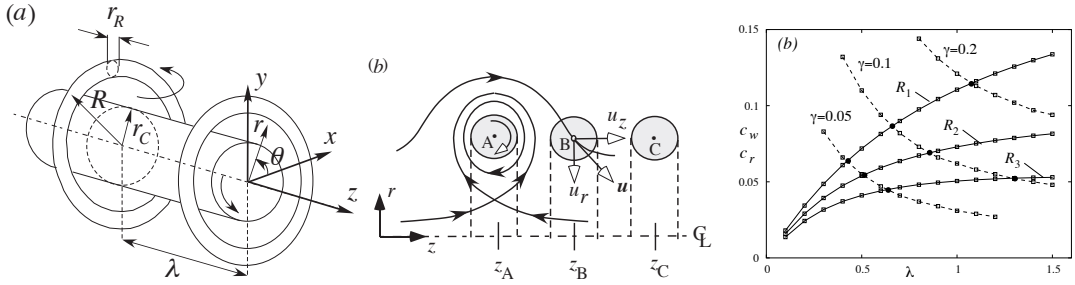


Figure 3: ($a$) Schematic of the initial condition. ($b$) Pattern of meridional streamlines induced by a thin-cored ring, showing how the mutually-induced velocity contributes to increased ring speed in a ring array. ($c$) Kelvin wave phase-speeds (solid curves) and ring speeds (dashed) for $\Gamma_R/\Gamma_c$ values of 0.05, 0.1, 0.15 and 0.2. Here $r_R = 0.05$, $r_C = 1$, $\Gamma_C = 1$.

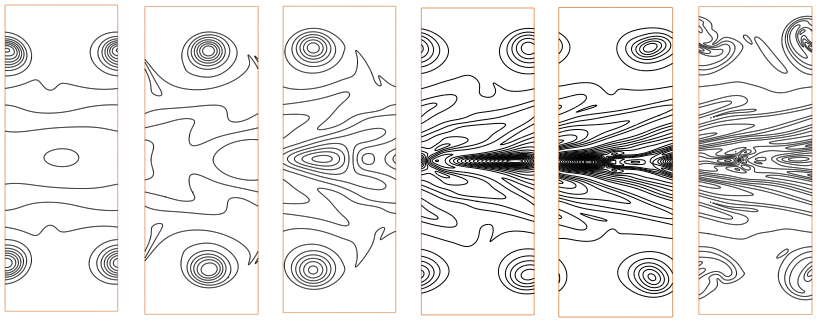

Figure 4: $\omega$ contours with levels $[0.2, 9., 0.4]$ for $\gamma = 0.2$ resonance at times $t = 5, 11, 19, 27, 37$ and 51. Here $Re = 10^4$ and $\lambda = 1.1$.

$u_r$ contribution coming from the ring at $z_C$, while the axial velocity contributions due to the rings at $z_A$ and $z_C$ are additive. With decreasing $\lambda$, the axial velocity contributions increase, and therefore so does $c_r$.

It is important to note that there are crossing-points of the $c_r$ and $c_w$ curves for small values of $\gamma$. At these points, the ring advection speed matches the phase speed of the CD wave of wavelength $\lambda$. Since the ring-induced perturbation in the column's core is periodic with wavelength $\lambda$, it can be expected that the rings will trigger a CD wave that travels at the same speed as each ring. Thus, one can expect resonance when the ring array has $\lambda$ that equals that at a crossing point.

In the following, we consider resonant growth at large $Re$, where the viscous arrest mechanism (i.e. the homogenization of the ring array) occurs sufficiently slowly for the core waves to grow to a very large magnitude. Here consider $\gamma = 0.2$ case (the relatively large $\gamma$ is unfortunately unavoidable due to numerical constraints, since the lower $\gamma$ cases require a $Re$ larger than that we can simulate.) $\omega$ contours in a meridional plane (Figure 4) show the generation of a rightward traveling CD wave and its growth. The advecting vorticity wavepacket in the core acquires a characteristic arrowhead shape, pointing in the upstream direction, similar to that observed in the case of CD on a polarized vortex column [1].

As the wave grows through resonance, its nonlinear self-interaction becomes increasingly important. There eventually comes a stage of evolution when the wave's amplitude growth results in a retardation of its wave-speed. This effect can be deduced from $\omega_z'$ evolutions plotted in figures $5(a, b)$. At the lower $Re$ (Figure $5a$), the $\omega_z'$ curves are nearly sinusoidal with a constant frequency and the evolutions at $z_0$ and $z_\pi$ remain out-of-phase throughout the period of growth. This behavior is characteristic of linear CD. At the higher $Re$ (Figure $5b$), the slower diffusion of the rings and the weaker dissipation of

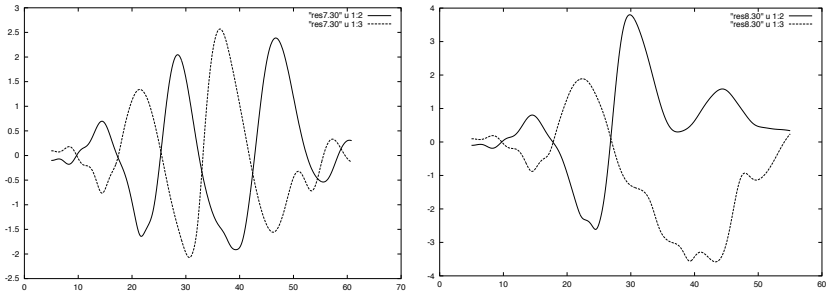


Figure 5: $\omega_z'$ evolution for $\gamma = 0.2$ resonance ($a$) $Re = 5000$ and ($b$) $Re = 10,000$. Solid curve is vorticity at $z_0$ and dashed at $z_\pi$. Here $\lambda = 1.1$.

core perturbation energy allow stronger growth of CD, over the same period of time as at $Re = 5000$. In this case, the CD wave's amplitude is sufficiently large for nonlinear effects to be significant. The retardation of the wave-speed is reflected in the reduced slopes of the $\omega_z'$ curves at late times (see the $z_\pi$ curve at $30 < t < 40$). Further, the vorticity wavepacket splits into two parts, and the advection of each packet past the $z_0$ plane is evident in the form of two successive maxima (at $t \approx 30$ and $t \approx 50$). These features of nonlinear core dynamics result from the self-advection term $w\partial\omega_\theta/\partial z$. Note that in linear CD both $w$ and $\omega_\theta$ are perturbation quantities. The nonlinear self-advection of the wave causes the matching between wave phase speed and the ring advection speed to be disrupted. Following such nonlinear detuning, resonant growth abruptly ceases (see Figure 4 at $t=51$).

## 3. TRANSIENT GROWTH OF PERTURBATIONS

Let us examine the role of transient growth during vortex turbulence interaction. We [3] have analyzed the linear-regime behavior of arbitrary small-amplitude perturbations to the Oseen vortex. The linear analysis established that (algebraically) growing perturbations exist and extracted those perturbations ("optimal modes") which maximize energy amplification, over a given time period of amplification $t$. "Globally-optimal" perturbations are defined as the optimal perturbations that maximize the amplification (referred to as the gain, $G(t) \equiv E(t)/E(0)$, where $E(t)$ is perturbation energy at time $t$) over all $t$, for a given set of parameter values: $m$, $k$ and $Re$; here $Re$ is the vortex Reynolds number, defined as circulation/viscosity.

Figure 6($a$) plots the globally maximal gains $G_{max}(k)$ for axisymmetric ($m = 0$) and bending wave ($m = 1$) modes. $G_{max}$ for $m = 0$ increases monotonically with decreasing $k$, attaining its largest value in the $k \to 0$ limit. The largest-growing modes are, however, also those with the smallest growth *rates*, with peak amplification attained at very large $t$. This is expected to limit the physical significance of these modes. While for most $k$ values, $m = 0$ modes have larger gains than $m = 1$ modes (Figure 6$a$), the bending wave optimals possess two features that give these modes prime significance in vortex-turbulence interaction: first, as seen above, $m = 1$ features large growth rates (compared to $m = 0$) and large gains (compared to $m > 1$ modes); second, bending wave modes grow through resonance with core waves, thereby exciting large fluctuations in the vortex core. This is seen in Figure 6($d$), where we plot the evolution of perturbation energy profiles. The core fluctuations attain levels far exceeding the perturbation amplitudes outside the core ($r > 1$). In contrast, perturbation energy in $m = 0$ modes remains localized near the radial location of the initial perturbation (Figure 6$c$). Thus, core transition (if it occurs) is likely to be the result of bending wave growth.

We evaluate the effects of nonlinearity by initializing the globally optimal perturbation at an amplitude of 6.6%. The simulation (Figure 7) is performed at vortex Reynolds number $Re \equiv \Gamma_0/\nu = 5000$. Initially the vorticity perturbation is located only outside the core (Figure 7$a, h$), with $\omega_\theta$ being small in comparison with $\omega_r$ and $\omega_z$. The strain field of the vortex column's swirl tilts $\omega_r$ into $\omega_\theta$ and

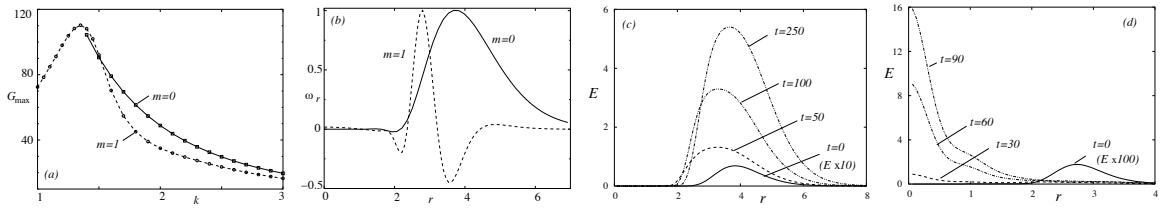


Figure 6: Results from linear analysis: ($a$) Globally maximal gain $G_{max}(k)$ for $m=0$ and $m=1$; ($b$) $\omega_r$ profiles for global optimals at $k = 1.5$; ($c$) Evolution of perturbation energy profiles $E(r)$ for $m=0$ mode in ($b$); ($d$) $E(r)$ profiles for $m=1$ mode in ($b$). In all cases, $Re = 5000$.

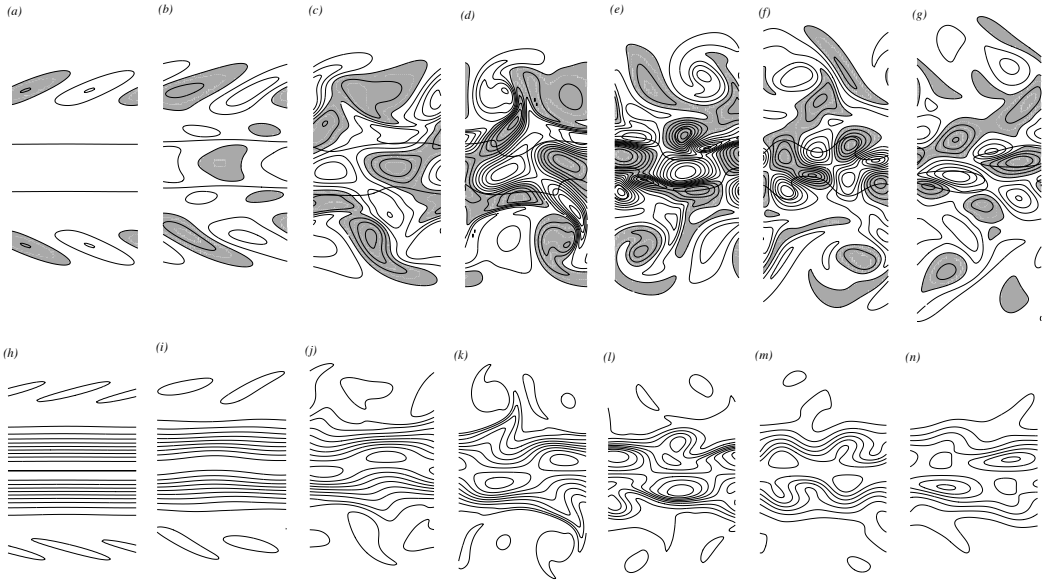

Figure 7: Contours of $\omega_y$ ($a$–$g$) and vorticity magnitude $\omega$ ($h$–$n$) in a meridional $x$-$z$ plane. Time shown are ($a, h$) $t = 0$, ($b, i$) $t = 10$, ($c, j$) $t = 20$, ($d, k$) $t = 30$, ($e, l$) $t = 50$, ($f, m$) $t = 75$, ($g, n$) $t = 100$. Shaded regions in ($a$-$g$) contain negative $\omega_y$. Contours plotted with increment $\delta\omega = 0.1$ in ($a$–$g$) and $\delta\omega = 0.2$ in ($h$–$n$). In ($a$–$g$) $\omega = 1$ contour is also shown to indicate the vortex core.

stretches the vorticity. The consequent growth of $\omega_\theta$ is seen in figures 7($b$–$d$). The external vorticity is organized into a spiral vortex filament ("thread"). The optimal mode's external $\omega_\theta$ is localized at a radius where the thread's induced velocity perturbation in the column's core can resonate with a bending wave eigenmode of the Oseen vortex. This leads to significant growth of core perturbation vorticity, whose magnitude soon exceeds that of the thread (Figure 7$d$). Note that the bending wave is associated with nearly equal magnitudes in all three vorticity components. In the meridional $x$-$z$ plane of Figure 7, the growth of $\omega_x$ (not shown) – which coincides with $\omega_r$ – causes appreciable deflection of the vortex column's axis; the deformation of the initially rectilinear column into a helical bending wave can be discerned in figures 7($d, k$).

The preceding mechanisms are essentially linear, but nonlinear effects strengthen progressively and are clear at larger times, $t > 30$. The most significant nonlinear effect is the roll-up of the external vorticity patches into vortex-like filaments. The self-induced motion of each segment of the spiral vortex filament advects the segment axially (along $z$). Further, the weaker $\omega_\theta$ cell located initially at smaller $r$ is wrapped around the stronger $\omega_\theta$ cell (Figure 7$d$). The net effect of the self-induced

motions of the threads (negligible in the linear limit) is that opposite-signed cells are organized into dipole-like structures. Mutual induction carries the dipole radially outwards (compare figures 7($c$) and figures 7($g$). The cumulative effect of transient growth is that flow appears to be nearly turbulent at late times. The development of a turbulence-like flow in a perturbed, *stable* vortex is remarkable. While no core transition is observed in the present case, vorticity isosurfaces (not shown) display significant distortion – with large-amplitude "twist" waves – of the initially cylindrical column. With increasing $Re$, core break-up into finer-scale filaments may very well occur since the transient amplifications increase with increasing $Re$. In practical flows, where $Re$ are about four orders of magnitude higher than in our simulation, core transition through transient excitation of bending waves appears to be a distinct possibility.

## 4. CONCLUDING REMARKS

To explain the enigmatic growth of core fluctuations in a "stable", rotating flow, we have analyzed two alternative mechanisms. The first – thread-vortex CD resonance – has been previously proposed in [2]. It has been found that there exist numerous "crossing points" where resonance is indeed possible between relatively weak rings and vortex CD waves traveling with the same celerity. The resonance can result in perturbation amplification by several orders-of-magnitude. No core transition has been seen however; this is perhaps due to the nonlinear detuning of the resonance as vortex CD waves lose speed with increasing amplitude as a result of nonlinear self-interaction. Further, analysis of turbulence statistics shows that the dominant modes in the vortex core are not axisymmetric, but bending, waves.

The second mechanism is the amplification of bending waves through resonant interaction with external turbulence filaments located at a critical radius outside the core. Such filaments are advected around the core with the same azimuthal velocity as the core bending wave, leading to a different kind of resonance and sustained amplification of the core wave [3]. Purusing mode evolution herein via DNS into the nonlinear regime, we find that perturbation growth results in significant core distortion and the appearance of turbulence-like finer-scale structures in the core periphery. The growth of even a single transient bending wave captures various aspects of turbulence statistics. Interestingly, a dominant bending wave mode appears to be adequate for accelerated vortex decay.

Nonlinear transient growth analysis appears to be the most tractable framework for understanding the evolution of turbulent vortices. Consistent with prior observations from experiments and simulations, the analysis predicts bending waves to be dominant perturbations in the core. Linear analysis in [3] shows that mode amplifications of several orders-of-magnitude is possible even at moderate $Re$. Detailed study of transient mode evolution is likely to suggest feasible means for vortex control in practical flows. These results suggest several avenues for further research, including the possibility of turbulence regeneration and self-sustenance, similar to that seen in wall-bounded shear flow, and the impact on long-term vortex decay; model-based prediction of vortex decay rates; and the relationship between transient growth and the growth of vortex modes when the external turbulence is forced.

Research funded by the National Science Foundation grant no. CBET-0554165.

## REFERENCES

[1] Melander MV and Hussain F. Polarized vortex dynamics on a vortex column. *Phys. Fluids A*, 1993. 5, 1992–2003.

[2] Miyazaki T and Hunt JCR. Linear and nonlinear interactions between a columnar vortex and external turbulence. *J. Fluid Mech.*, 2000. 402, 349–378.

[3] Pradeep DS and Hussain F. Transient growth of perturbations in a stable vortex. *J. Fluid Mech.*, 2006. 550, 251–288.